Diagenetic effects on strontium isotope (^{87}Sr/^{86}Sr) and elemental (Sr, Mn, and Fe) signatures of Late Ordovician carbonates

Dongping Hu[1] ✉, Dandan Li[1], Lian Zhou[2], Lilin Sun[1], and Yilun Xu[1]
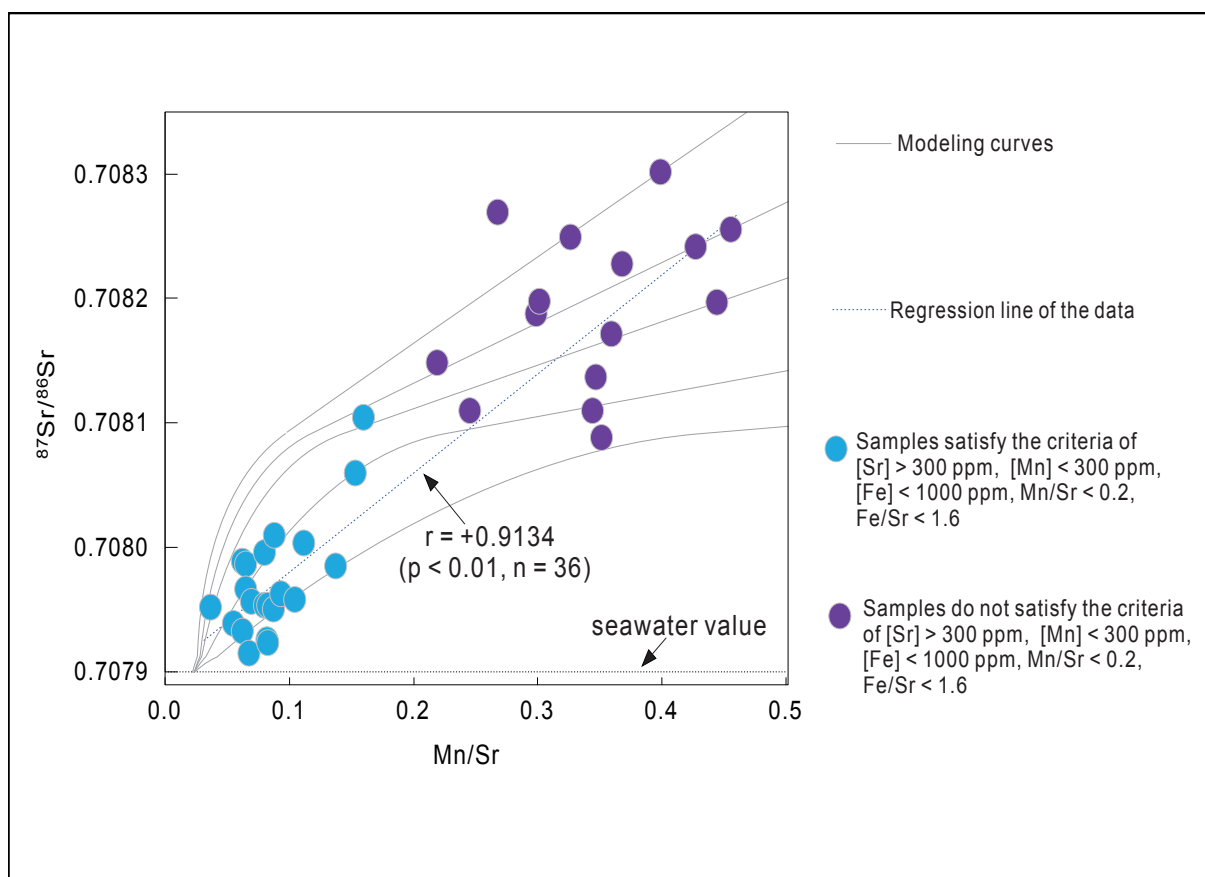
[1]*School of Earth and Space Sciences, University of Science and Technology of China, Hefei 230026, China;*
[2]*State Key Laboratory of Geological Processes and Mineral Resources, China University of Geosciences, Wuhan 430074, China*

✉Correspondence: Dongping Hu, E-mail: hudp08@mail.ustc.edu.cn

Graphical abstract

^{87}Sr/ ^{86}Sr of carbonates can still be diagenetically altered although the samples meet the stricter geochemical criteria of retention.

Public summary

■ The Monitor Range section records significantly higher ^{87}Sr/^{86}Sr values than the coeval seawater.

■ The radiogenic ^{87}Sr/^{86}Sr ratios can be fully attributed to diagenetic alteration.

■ A comprehensive approach that incorporates evaluation of ^{87}Sr/^{86}Sr correlations with diagenetic indicators and numerical simulation is proposed to identify the primary seawater Sr isotope signal.

Diagenetic effects on strontium isotope (⁸⁷Sr/⁸⁶Sr) and elemental (Sr, Mn, and Fe) signatures of Late Ordovician carbonates

Dongping Hu[1] ✉, Dandan Li[1], Lian Zhou[2], Lilin Sun[1], and Yilun Xu[1]

[1]*School of Earth and Space Sciences, University of Science and Technology of China, Hefei 230026, China;*
[2]*State Key Laboratory of Geological Processes and Mineral Resources, China University of Geosciences, Wuhan 430074, China*

✉Correspondence: Dongping Hu, E-mail: hudp08@mail.ustc.edu.cn

Cite This: *JUSTC*, **2023**, 53(5): 0503 (9pp)   Read Online

Abstract: Understanding the effect and extent of diagenesis on the isotopic compositions of Sr in marine carbonates is a critical prerequisite for their use to unravel past environments. Here, we explore the dominant controls on carbonate ⁸⁷Sr/⁸⁶Sr of a Late Ordovician section from the Monitor Range, USA. Our results reveal a distinct increase in ⁸⁷Sr/⁸⁶Sr from 0.70794 to 0.70830 in the mid-upper *D. ornatus* zone, which is markedly higher than the published datasets of contemporaneous samples with a relatively lower and stable ⁸⁷Sr/⁸⁶Sr ratio of ~0.7079. These elevated ⁸⁷Sr/⁸⁶Sr ratios suggest a local and post-depositional overprint and cannot be interpreted to reflect the ⁸⁷Sr/⁸⁶Sr of the coeval seawater. Furthermore, ⁸⁷Sr/⁸⁶Sr exhibits statistically significant positive correlations with geochemical indicators for diagenesis ([Mn], [Fe], Mn/Sr, Fe/Sr), indicating that diagenetic alteration is the principal control on the observed radiogenic ⁸⁷Sr/⁸⁶Sr values. Using a numerical model of marine diagenetic fluid-rock interaction, we demonstrate that the observed Sr isotopic and elemental data can be best explained by the chemical variations in bulk carbonates associated with diagenetic alteration. Our results highlight that diagenesis may significantly alter the pristine ⁸⁷Sr/⁸⁶Sr ratios of carbonates than previously thought, although the samples satisfy the stricter geochemical criteria of Sr isotope preservation ([Sr] > 300 ppm, [Mn] < 300 ppm, [Fe] < 1000 ppm, Mn/Sr < 0.2, Fe/Sr < 1.6), pointing to the need for more caution when using bulk carbonate ⁸⁷Sr/⁸⁶Sr as a tracer of paleoenvironmental changes.

Keywords: strontium isotopes; bulk carbonates; Late Ordovician; diagenetic alteration

CLC number: P597⁺.2   **Document code:** A

1 Introduction

The ubiquitous deposition of sedimentary carbonates along passive continental margins over the last 3.8 billion years provides the potential for long-term, continuous, and high-resolution records of past environmental conditions[1]. These records can be examined by geochemical analyses of carbonates based on their stable isotope compositions (e.g., δ¹³C, δ¹⁸O, δ²³⁸U) and/or trace element contents (e.g., I/Ca, Ce/Ce*)[2−5]. In particular, carbonate strontium isotope (⁸⁷Sr/⁸⁶Sr) records could offer important constraints on the magnitude and timing of continental weathering, paleoclimate changes, and tectonic activities in the geological past[6−14]. In addition, ⁸⁷Sr/⁸⁶Sr stratigraphy has long been used as a chemostratigraphic technique to correlate strata over the last billion years[15−19], especially when biostratigraphic data are deficient or unavailable. However, multiple factors can influence the extent to which the ⁸⁷Sr/⁸⁶Sr of bulk carbonates traces the seawater Sr isotope compositions at the time of deposition; for instance, post-depositional diagenesis is the most prevalent and significant mechanism that could alter the primary ⁸⁷Sr/⁸⁶Sr signatures of carbonate[15, 20−22]. As a result, diagenetic alteration must be carefully assessed prior to interpreting carbonate ⁸⁷Sr/⁸⁶Sr as records of secular changes in seawater ⁸⁷Sr/⁸⁶Sr.

The mid-late Katian immediately before the Hirnantian glaciation (latest Ordovician) is an excellent time interval during which to investigate the major controls on ⁸⁷Sr/⁸⁶Sr of bulk carbonates because large published datasets have shown a relatively stable and lower seawater ⁸⁷Sr/⁸⁶Sr value of ~0.7079[6, 15, 16]. This low ⁸⁷Sr/⁸⁶Sr ratio has commonly been attributed to enhanced weathering of fresh volcanic rocks, leading to a more juvenile seawater ⁸⁷Sr/⁸⁶Sr value, as well as lowering of atmospheric CO₂ levels, global cooling, and the first significant ice age of the Phanerozoic (Hirnantian glaciation, ca. 443 Ma)[6, 11, 23, 24]. Thus, if the observed coeval ⁸⁷Sr/⁸⁶Sr records do not coincide with this value (i.e., ~0.7079), then other factors must have been involved to change the primary ⁸⁷Sr/⁸⁶Sr of the studied samples.

In this study, we examined the ⁸⁷Sr/⁸⁶Sr and elemental concentrations of Sr, Mn and Fe ([Sr], [Mn], [Fe]) in bulk carbonate rocks from the Monitor Range section situated in central Nevada, USA. We focus on this locality because it provides continuous and undisturbed Late Ordovician sedimentary records with well-established biochronological and geochemical data[25−28], offering a promising opportunity to explore the potential factors that could have modified the original ⁸⁷Sr/⁸⁶Sr signals of carbonate. We develop a fluid-rock interaction modeling to further evaluate the resetting of ⁸⁷Sr/⁸⁶Sr

and elemental concentrations of Sr, Mn, and Fe during post-depositional diagenesis and compare the model predictions with observed records to demonstrate how incorporating geochemical data alongside diagenetic model results can support the identification of pristine seawater $^{87}Sr/^{86}Sr$ ratios.

2 Geological settings

The Monitor Range section (39°12.660'N, 116°24.257'W), in north-central Nevada, USA, is exceptionally exposed and allows high-resolution collection of samples spanning the Katian-Hirnantian interval. Previous studies of this section have established a robust stratigraphic framework, including biostratigraphy, sedimentology, and chemostratigraphy[25−32]. The biostratigraphy, based mainly on graptolites, is well constrained and composed of the *D. ornatus* and *P. pacificus* zones in ascending order for the Katian stage (Fig. 1). These biozones can be correlated regionally and globally with coeval successions[25, 26].

Sedimentologically, the *D. ornatus* zone consists mainly of clayey lime mudstone to brown-gray to dark brown calcareous mudstone interbedded with dark gray lime mudstone (Fig. 1). The overlying lower-middle *P. pacificus* zone is dominated by the lithology of thin- to medium-bedded dark gray lime mudstone and interbeds of clayey lime mudstone to calcareous mudstone. Stratigraphically higher, the upper part

of the *P. pacificus* zone is composed predominantly of medium- to thick-bedded lime mudstone interbedded with thin calcareous mudstone and chert nodules, blebs, bulbous, and stringers.

3 Methods

3.1 Sample preparation

A total of 36 bulk carbonate samples spanning the mid-late Katian from the Monitor Range section are washed thoroughly with deionized water to remove surface contaminants and sliced into small pieces or chips to remove any visually weathered parts and altered materials. The dried sample pieces were then pulverized into powder (< 200 mesh) using a vibratory disc mill for geochemical analyses.

3.2 Analyses of elemental concentrations and $^{87}Sr/^{86}Sr$

Approximately 0.12 g of each sample was dissolved in 30% acetic acid using a 10-mL precleaned centrifuge tube at room temperature to avoid dissolution of noncarbonate phases. The samples were then centrifuged to separate the supernatant from insoluble residues. Aliquots of clear supernatant were evaporated to dryness and brought up in 2% HNO_3 for elemental concentration analyses on an ICP AES instrument. Typical precision was better than 10% (2σ) based on
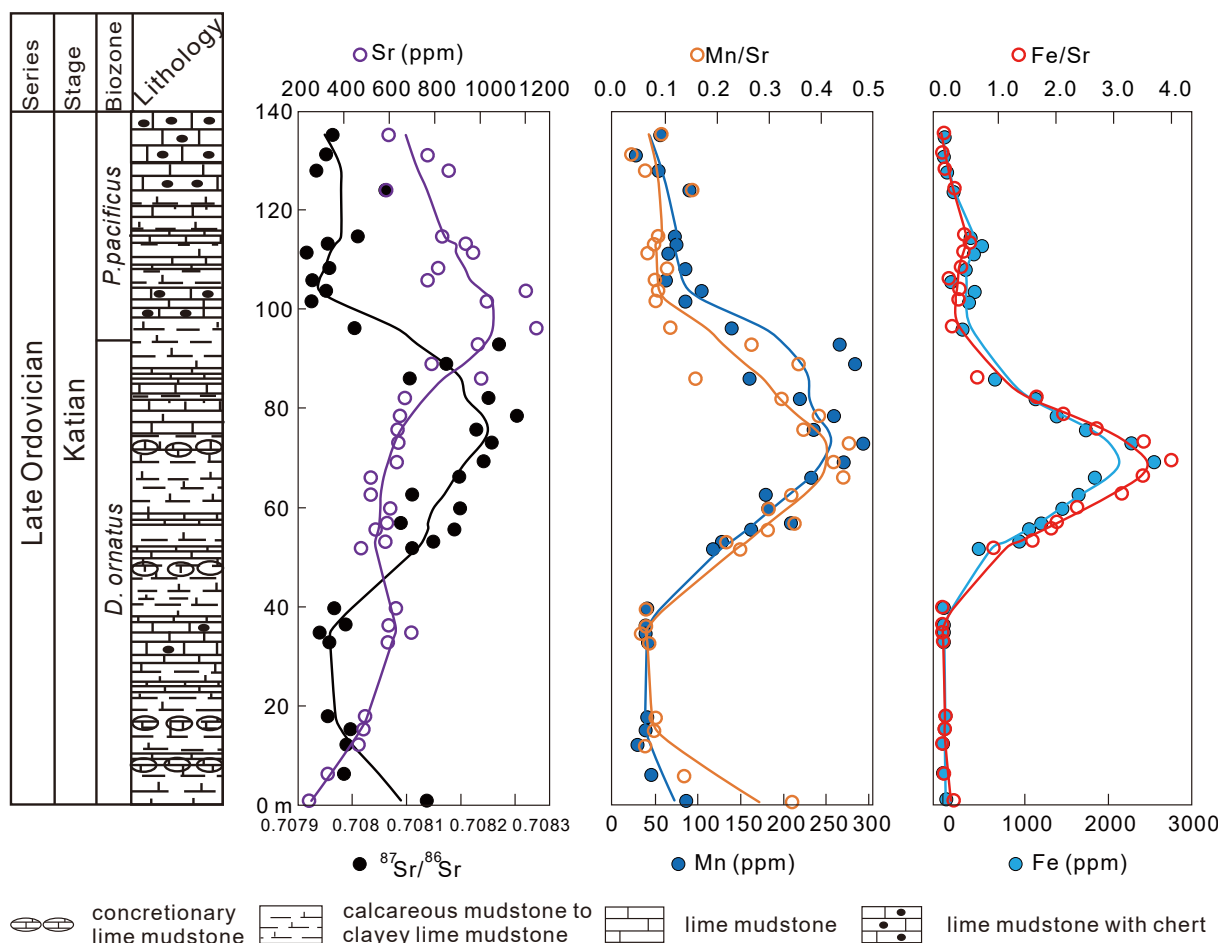

Fig. 1. Lithological, $^{87}Sr/^{86}Sr$, [Sr], [Mn], Mn/Sr, [Fe], and Fe/Sr profiles of the Monitor Range section. Graptolite biostratigraphy and lithostratigraphy are based on Finney et al. [26]. Solid curves are the locally weighted scatterplot smoothing (LOWESS) fits for the geochemical data.

duplicate analyses of in-run check standards.

For the $^{87}Sr/^{86}Sr$ measurements, the sample supernatants were dried completely and taken up in 2.5 mol/L HCl for Sr purification. Purification of Sr was conducted following standard cation-exchange procedures[33]. The $^{87}Sr/^{86}Sr$ of purified samples was measured on a Thermo Scientific Triton thermal ionization mass spectrometer. The reported $^{87}Sr/^{86}Sr$ ratios were corrected for instrumental mass discrimination using a normal Sr ratio of $^{86}Sr/^{88}Sr = 0.1194$, with typical precision better than 0.00001 (2σ).

4 Results

We observed distinct stratigraphic variations in $^{87}Sr/^{86}Sr$ and elemental concentrations (i.e., [Sr], [Mn], [Fe]) in the Monitor Range section (Fig. 1, Table 1). The $^{87}Sr/^{86}Sr$ in the lower *D. ornatus* zone declines from 0.70814 to 0.70794 over the interval of 0–34.7 m. Synchronously, [Sr] increases from 257.0 ppm to 700.6 ppm, accompanied by relatively low concentrations of Mn and Fe, thus resulting in low ratios of Mn/Sr and Fe/Sr in this interval. $^{87}Sr/^{86}Sr$ then rises

Table 1. $^{87}Sr/^{86}Sr$ and elemental data from the Monitor Range section, Nevada, USA.

Sample	Stage	Biozone	$^{87}Sr/^{86}Sr$	$\pm 2\sigma$	Sr (ppm)	Mn (ppm)	Fe (ppm)	Mn/Sr	Fe/Sr	Height (m)
MRS-111	Katian	*P. pacificus*	0.707963	0.000001	600.1	55.6	35.5	0.09	0.06	135.1
MRS-109	Katian	*P. pacificus*	0.707952	0.000006	770.8	27.6	30.1	0.04	0.04	131.1
MRS-106	Katian	*P. pacificus*	0.707933	0.000009	865.6	53.5	67.2	0.06	0.08	127.9
MRS-102	Katian	*P. pacificus*	0.708060	0.000004	589.0	89.9	147.6	0.15	0.25	124.0
MRS-100	Katian	*P. pacificus*	0.708010	0.000005	835.1	73.2	343.9	0.09	0.41	114.7
MRS-98	Katian	*P. pacificus*	0.707954	0.000005	939.2	74.5	485.4	0.08	0.52	113.1
MRS-95	Katian	*P. pacificus*	0.707915	0.000005	971.3	65.1	390.5	0.07	0.40	111.3
MRS-91	Katian	*P. pacificus*	0.707958	0.000004	816.8	85.0	292.6	0.10	0.36	108.2
MRS-89	Katian	*P. pacificus*	0.707926	0.000006	771.6	62.6	113.9	0.08	0.15	105.8
MRS-86	Katian	*P. pacificus*	0.707951	0.000006	1205.2	104.3	400.4	0.09	0.33	103.7
MRS-83	Katian	*P. pacificus*	0.707924	0.000008	1034.6	84.9	324.7	0.08	0.31	101.6
MRS-79	Katian	*P. pacificus*	0.708004	0.000006	1251.7	138.9	249.6	0.11	0.20	96.2
MRS-74	Katian	*D. ornatus*	0.708270	0.000006	993.6	265.9	–	0.27	–	92.9
MRS-71	Katian	*D. ornatus*	0.708172	0.000006	790.4	283.8	–	0.36	–	89.0
MRS-67	Katian	*D. ornatus*	0.708105	0.000006	1006.7	160.4	641.4	0.16	0.64	86.0
MRS-64	Katian	*D. ornatus*	0.708250	0.000005	671.1	218.7	1124.1	0.33	1.68	82.0
MRS-61	Katian	*D. ornatus*	0.708302	0.000005	648.6	258.3	1384.2	0.40	2.13	78.5
MRS-57	Katian	*D. ornatus*	0.708228	0.000005	638.8	234.8	1734.9	0.37	2.72	75.7
MRS-53	Katian	*D. ornatus*	0.708256	0.000006	643.7	293.0	2270.9	0.46	3.53	73.0
MRS-49	Katian	*D. ornatus*	0.708242	0.000005	634.7	270.6	2548.4	0.43	4.02	69.2
MRS-45	Katian	*D. ornatus*	0.708197	0.000006	522.4	231.9	1840.0	0.44	3.52	66.1
MRS-41	Katian	*D. ornatus*	0.708110	0.000004	521.9	179.4	1643.3	0.34	3.15	62.6
MRS-37	Katian	*D. ornatus*	0.708198	0.000004	606.1	182.3	1443.9	0.30	2.38	59.8
MRS-34	Katian	*D. ornatus*	0.708089	0.000004	593.7	208.5	1198.5	0.35	2.02	56.9
MRS-32	Katian	*D. ornatus*	0.708188	0.000006	543.2	162.0	1049.5	0.30	1.93	55.6
MRS-28	Katian	*D. ornatus*	0.708149	0.000005	584.9	127.9	935.6	0.22	1.60	53.1
MRS-25	Katian	*D. ornatus*	0.708110	0.000005	479.2	117.4	441.7	0.25	0.92	51.7
MRS-24	Katian	*D. ornatus*	0.707967	0.000005	632.8	40.6	23.4	0.06	0.04	39.7
MRS-19	Katian	*D. ornatus*	0.707987	0.000004	597.9	38.3	23.6	0.06	0.04	36.3
MRS-16	Katian	*D. ornatus*	0.707939	0.000004	700.6	38.1	26.9	0.05	0.04	34.7
MRS-12	Katian	*D. ornatus*	0.707957	0.000004	595.1	41.2	25.7	0.07	0.04	32.8
MRS-11	Katian	*D. ornatus*	0.707954	0.000004	496.8	40.8	42.5	0.08	0.09	17.8
MRS-9	Katian	*D. ornatus*	0.707996	0.000004	488.2	38.7	36.1	0.08	0.07	15.2
MRS-7	Katian	*D. ornatus*	0.707989	0.000004	466.5	28.9	19.5	0.06	0.04	12.2
MRS-5	Katian	*D. ornatus*	0.707985	0.000004	332.4	45.4	20.4	0.14	0.06	6.2
MRS-1	Katian	*D. ornatus*	0.708137	0.000005	248.1	85.9	59.1	0.35	0.24	0.9

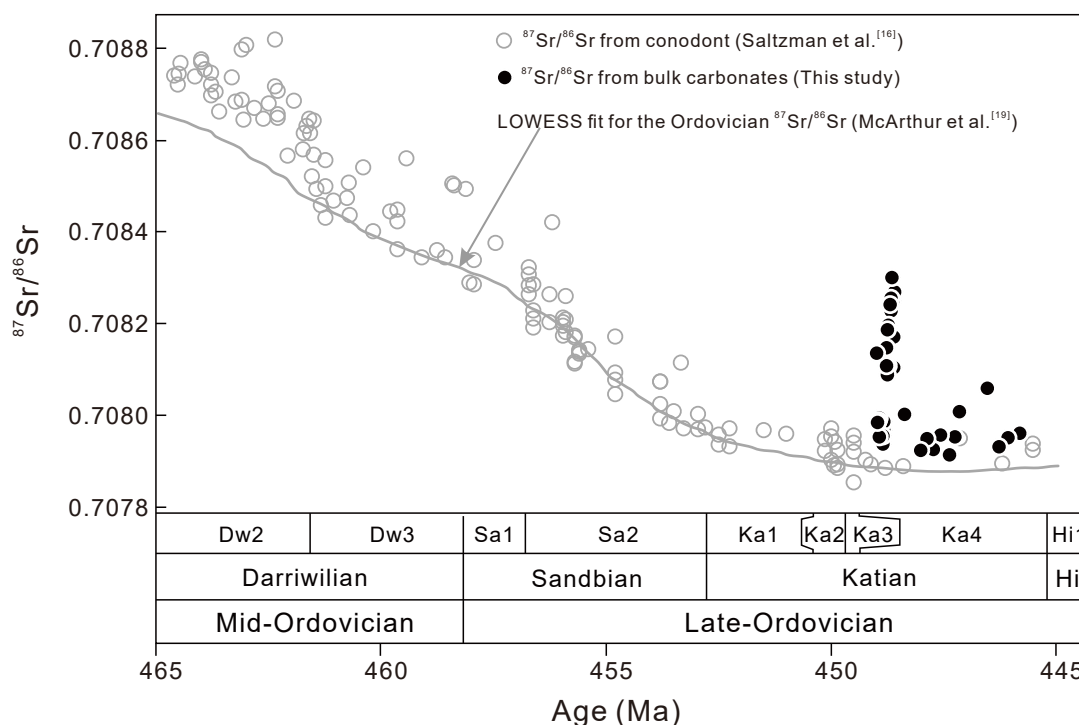**Fig. 2.** Comparison of carbonate $^{87}Sr/^{86}Sr$ records in the present study with published datasets derived from conodonts. The gray solid line is the LOWESS curve of $^{87}Sr/^{86}Sr$ datasets from Qing et al.[43], Shields et al.[44], Saltzman et al.[16], and Edwards et al.[15], representing the best fit for the published Ordovician $^{87}Sr/^{86}Sr$ data[19]. The time scale of the Ordovician is based on *Geologic Time Scale 2020*[34], and the stage slices are from Bergström et al.[45]. Hi.: Hirnantian.

continuously in the middle *D. ornatus* zone and reaches a maximum of 0.70830 at 78.5 m. This increase in $^{87}Sr/^{86}Sr$ coincides with an overall decline in [Sr], showing a roughly reverse stratigraphic trend of the two. Additionally, the [Mn], [Fe], Mn/Sr, and Fe/Sr ratios display congruent increasing trends in the corresponding interval.

The $^{87}Sr/^{86}Sr$ then returned to a lower ratio of 0.70792 at 101.6 m at the top of the *D. ornatus* zone. Again, [Sr] displays an increasing trend coincident with prominent decreases in the [Mn], [Fe], Mn/Sr, and Fe/Sr ratios in this interval. Higher section, $^{87}Sr/^{86}Sr$ shows limited variations between 0.70792 and 0.70806 at the *P. pacificus* zone over the interval of 103.7–135.1 m, coinciding with lower and stable values of [Mn], [Fe], Mn/Sr, and Fe/Sr. We note that the Mn/Sr ratios are consistently very low, falling below 0.4 in almost all of the data and averaging approximately 0.19 (Table 1, Fig. 1).

5 Discussion

5.1 Comparison with the published Katian $^{87}Sr/^{86}Sr$ datasets

To evaluate the validity of our newly obtained Sr isotope record from the Monitor Range section, we compared them with the published coeval $^{87}Sr/^{86}Sr$ datasets after calibration to the age framework based on *Geologic Time Scale 2020*[34]. Sixteen out of 36 $^{87}Sr/^{86}Sr$ values from the Monitor Range section vary between 0.70808 and 0.70830, showing a remarkable offset (with an average of 0.00029) with the coeval seawater $^{87}Sr/^{86}Sr$ ratio of ~0.7079[16, 19] (Fig. 2). These anomalously radiogenic values suggest that local effects have shifted

the primary Sr isotopic signals and thus cannot represent the secular changes in $^{87}Sr/^{86}Sr$ of global seawater.

5.2 Controls on $^{87}Sr/^{86}Sr$ records of the Monitor Range section

Carbonates from geological records have suffered various degrees of diagenetic alteration since their deposition, which is the most common factor that can modulate the $^{87}Sr/^{86}Sr$ ratios and the degree to which they track the variations in coeval seawater $^{87}Sr/^{86}Sr$[10, 20–22, 35]. During diagenesis, the trace element concentrations of carbonates would change systematically with the importation of foreign Sr, which could significantly alter the original $^{87}Sr/^{86}Sr$. To evaluate the importance of diagenesis that may influence the $^{87}Sr/^{86}Sr$ records at the Monitor Range section, we examined the [Sr], [Mn], [Fe], Mn/Sr, and Fe/Sr ratios (Fig. 3). [Mn], [Fe], Mn/Sr, and Fe/Sr ratios are important for evaluating the preservation of carbonate $^{87}Sr/^{86}Sr$ values, as Mn and Fe can act as tracers of nonmarine diagenetic fluids, such as continental, meteoric, and metamorphic fluids, which are commonly characterized by higher Mn and Fe concentrations and radiogenic $^{87}Sr/^{86}Sr$ ratios[21, 22, 35, 36]. Post-depositional diagenetic processes commonly result in high $^{87}Sr/^{86}Sr$ ratios along with an enrichment of Mn and Fe and depletion of Sr in the final carbonates[10, 20–22, 35, 37], as Mn and Fe have larger partition coefficients, leading to preferential incorporation into carbonate from diagenetic fluids[22, 37, 38]. The diagenetically altered carbonates, therefore, may be theoretically expected to have higher [Mn] and [Fe] with lower [Sr] and thus higher Mn/Sr and Fe/Sr ratios than the primary phase[10, 20–22]. Hence, the comprehensive study of $^{87}Sr/^{86}Sr$ with [Mn], [Sr], and [Fe] is
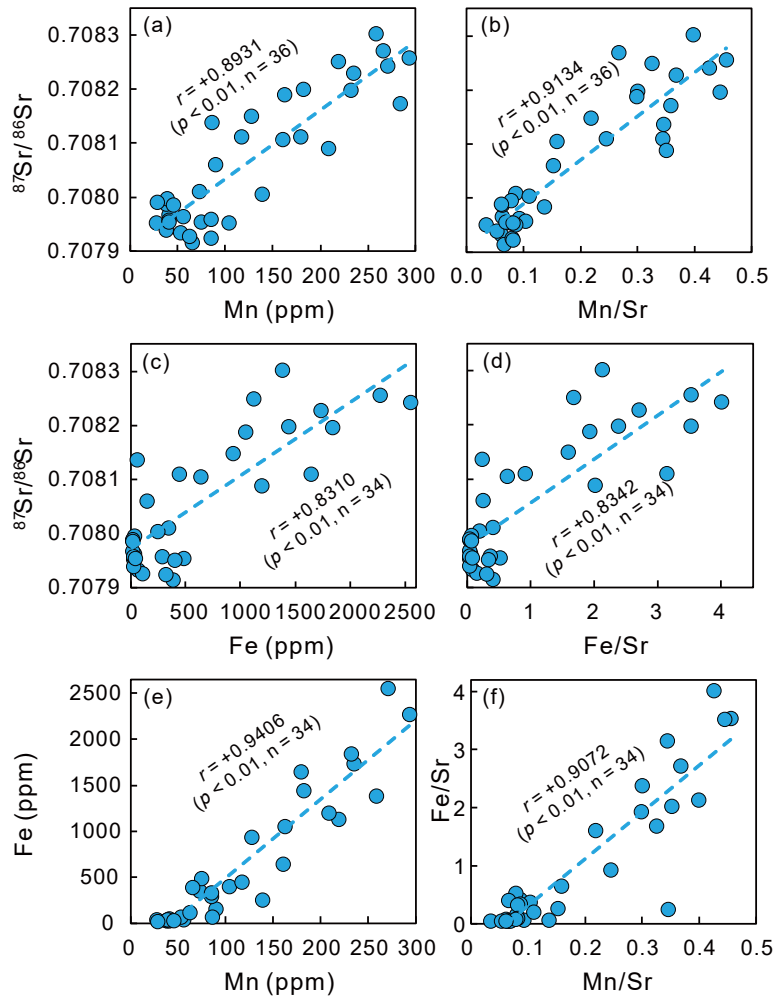
Fig. 3. Crossplots of (a) $^{87}Sr/^{86}Sr$ versus [Mn], (b) $^{87}Sr/^{86}Sr$ versus Mn/Sr, (c) $^{87}Sr/^{86}Sr$ versus [Fe], (d) $^{87}Sr/^{86}Sr$ versus Fe/Sr, (e) [Mn] versus [Fe], and (f) Mn/Sr versus Fe/Sr from the Monitor Range section. r represents the correlation coefficient. Note that all six crossplots show statistically significant positive correlations.

promising to assess the intensity of post-sedimentation alteration on the original $^{87}Sr/^{86}Sr$ of carbonates[38, 39].

Previous studies have attempted to use [Sr], [Mn], [Fe], Mn/Sr, and Fe/Sr values as geochemical criteria for identifying the least altered carbonates. For instance, Burke et al. [18] constructed the Phanerozoic $^{87}Sr/^{86}Sr$ curve by using bulk carbonates with [Sr] > 200 ppm, and Denison et al. [35] used the values of [Sr] > 900 ppm, [Mn] < 300 ppm, and Mn/Sr < 0.5 for late Paleozoic shelf carbonates. Edwards et al. [15] analyzed the paired $^{87}Sr/^{86}Sr$ of well-preserved conodont apatite and bulk carbonates from the Ordovician and suggested that the original seawater $^{87}Sr/^{86}Sr$ can be faithfully recorded in bulk carbonate with [Sr] > 300 ppm, and Wang et al. [40] proposed that samples with [Mn] < 300 ppm, [Fe] < 1000 ppm, and Mn/Sr < 1 are capable of preserving signals of Permian seawater $^{87}Sr/^{86}Sr$. When including the Fe/Sr ratios, Kuznetsov et al. [41] suggested that carbonates are likely to preserve the primary Sr isotopic composition if Mn/Sr < 0.2 and Fe/Sr < 5, and Rud'ko et al. [42] evaluated the $^{87}Sr/^{86}Sr$ of Upper Jurassic carbonates under stricter values of Mn/Sr < 0.2 and Fe/Sr < 1.6. Collectively, [Sr] > 300 ppm, [Mn] < 300 ppm, [Fe] < 1000 ppm, Mn/Sr < 0.2, and Fe/Sr < 1.6 can be considered as more severe and stricter geochemical criteria for Sr isotope

preservation in Ordovician carbonate rocks.

In the Monitor Range section, all the samples have [Sr] > 300 ppm and vary between 332.4 and 1251.7 ppm with an average of 709.7 ppm ($n = 35$), except for a value of 248.1 ppm obtained in one sample at the base of the studied section (Fig. 1, Table 1). [Mn] is lower than 300 ppm and ranges from 27.6 to 293.0 ppm, with a mean of 125.2 ppm ($n = 36$). Twenty-four out of 34 samples have [Fe] < 1000 ppm and range from 19.5 to 2548.4 ppm with an average of 629.9 ppm ($n = 34$) (Figs. 1 and 3, Table 1). Correspondingly, the Mn/Sr of the Monitor Range section exhibits low values ranging from 0.04 to 0.46 with a mean of 0.19, while Fe/Sr ranges from 0.04 to 4.02 with a mean of 1.00 (Table 1). On the basis of the abovementioned geochemical criteria of preservation of the Sr isotope system in Ordovician limestones (i.e., [Sr] > 300 ppm, [Mn] < 300 ppm, [Fe] < 1000 ppm, Mn/Sr < 0.2, Fe/Sr < 1.6), the $^{87}Sr/^{86}Sr$ of the samples from the Monitor Range section with [Fe] > 1000 ppm, Fe/Sr > 1.6, and Mn/Sr > 0.2 may be considered to have been diagenetically altered.

Although some samples meet the geochemical criteria, their $^{87}Sr/^{86}Sr$ values are still higher than that of coeval seawater (~0.7079, Fig. 2), suggesting that diagenesis or other post-depositional processes remain the dominant controls on the

observed $^{87}\text{Sr}/^{86}\text{Sr}$. To further check whether these elevated $^{87}\text{Sr}/^{86}\text{Sr}$ ratios could be interpreted entirely by diagenetic alteration, we dissect the correlations of $^{87}\text{Sr}/^{86}\text{Sr}$ with [Mn], [Fe], Mn/Sr, and Fe/Sr (Fig. 3). The scatter plots of $^{87}\text{Sr}/^{86}\text{Sr}$ vs. [Mn], Mn/Sr, [Fe], and Fe/Sr all show statistically significant positive correlations ($p < 0.01$, $r = +0.8931$, $+0.9134$, $+0.8310$, and $+0.8342$, respectively; Fig. 3a–d). Furthermore, the correlations of [Mn] with [Fe] and Mn/Sr with Fe/Sr are also significant ($p < 0.01$, $r = +0.9406$, $+0.9072$, respectively; Fig. 3e–f). These positive correlations are consistent with the prediction of $^{87}\text{Sr}/^{86}\text{Sr}$ trends to higher values with depletion of Sr and enrichment of Mn and Fe during diagenetic alteration[15, 21, 35, 39]. Collectively, we suggest that diagenetic resetting is likely to fully account for the radiogenic $^{87}\text{Sr}/^{86}\text{Sr}$ ratios of bulk carbonates from the Monitor Range section.

6 Developing a theoretical model for $^{87}\text{Sr}/^{86}\text{Sr}$ variation during carbonate diagenesis

To more systematically and quantitatively constrain the influence of diagenetic alteration on the $^{87}\text{Sr}/^{86}\text{Sr}$ records at the Monitor Range, we develop a numerical open system fluid-rock interaction model that involves the evolution of [Sr], [Mn], [Fe], Mn/Sr, Fe/Sr, and $^{87}\text{Sr}/^{86}\text{Sr}$ ratios during carbonate diagenesis to interpret the observed trends[20, 21]. In this model, the concentration of element i (e.g., Mn, Sr, Fe) in the carbonate (C_i^r) is expressed using the following equation:

$$C_i^r = D_i C_i^{f0} + (C_i^{r0} - D_i C_i^{f0}) \exp\left(-\frac{N}{D_i}\right), \qquad (1)$$

where C_i^{r0} and C_i^{f0} are the initial concentrations of element i in the carbonates and fluid, respectively. D_i is the effective fluid-rock distribution coefficient and is defined by the ratio of C_i^r to C_i^f (i.e., $D_i = C_i^r/C_i^f$). N is the weight ratio of fluid to carbonate.

The final strontium isotopic composition of carbonate ($(^{87}\text{Sr}/^{86}\text{Sr})^r$) is a function of the ratio of the initial Sr concentration in carbonates (C_{Sr}^{r0}) to that in fluid (C_{Sr}^{f0}), the initial $^{87}\text{Sr}/^{86}\text{Sr}$ isotope ratio of carbonates ($(^{87}\text{Sr}/^{86}\text{Sr})^{r0}$) and fluid ($(^{87}\text{Sr}/^{86}\text{Sr})^{f0}$), the effective fluid-rock distribution coefficient (D_{Sr}), and the weight ratio of fluid to carbonate (N), which is described by the following formula:

$$(^{87}\text{Sr}/^{86}\text{Sr})^r = \frac{\left(\frac{C_{\text{Sr}}^{r0}}{C_{\text{Sr}}^{f0}}\right)(^{87}\text{Sr}/^{86}\text{Sr})^{r0} + (^{87}\text{Sr}/^{86}\text{Sr})^{f0} D_{\text{Sr}}\left[\exp\left(\frac{N}{D_{\text{Sr}}}\right) - 1\right]}{\left(\frac{C_{\text{Sr}}^{r0}}{C_{\text{Sr}}^{f0}}\right) + D_{\text{Sr}}\left[\exp\left(\frac{N}{D_{\text{Sr}}}\right) - 1\right]}. \qquad (2)$$

The modeling outputs are illustrated in Figs. 4 and 5, providing a theoretical basis for the evolution of $^{87}\text{Sr}/^{86}\text{Sr}$ with [Sr], [Mn], [Fe], Mn/Sr, and Fe/Sr. The element concentrations in fluid (C_i^{f0}) used in this model are variable to capture a broader significance for the natural burial environments. For fluids with relatively high Sr concentrations, such as Sr-rich brine (e.g., $C_{\text{Sr}}^{r0}/C_{\text{Sr}}^{f0} < 10$), the $^{87}\text{Sr}/^{86}\text{Sr}$ of carbonates could be easily altered via fluid-rock interactions with low fluid-to-rock ratios ($N < 1$, Fig. 4a). Our model predicts that $^{87}\text{Sr}/^{86}\text{Sr}$ would increase simultaneously with increasing [Mn], [Fe], Mn/Sr, and Fe/Sr ratios during diagenesis of carbonates (Fig. 5). When applying the modeling results to the studied samples, the observed covariations between $^{87}\text{Sr}/^{86}\text{Sr}$ and diagenetic indicators ([Mn], [Fe], Mn/Sr, Fe/Sr) can be largely reproduced through fluid-rock interactions (Fig. 6), further supporting that the anomalously radiogenic $^{87}\text{Sr}/^{86}\text{Sr}$ values in the Monitor Range section can be best explained by diagenetic alteration.

7 Implications of carbonate diagenesis for the Sr isotope paleoenvironmental proxy

Our results have two substantial implications for the explanation of Sr isotopic records in geological carbonates. First, our results demonstrate that post-depositional diagenesis can result in significant stratigraphic variations in $^{87}\text{Sr}/^{86}\text{Sr}$ of carbonate rocks that do not represent primary changes in isotopic
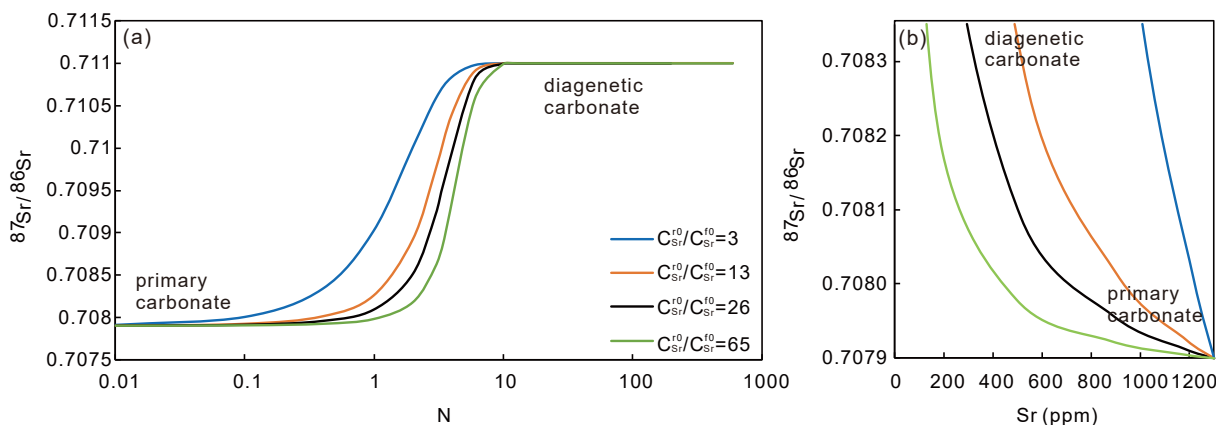

Fig. 4. Modeling results illustrating the evolution of carbonate $^{87}\text{Sr}/^{86}\text{Sr}$ versus the weight ratio of fluid to rock (N) and [Sr] during fluid-rock interactions in an open system condition. (a) $^{87}\text{Sr}/^{86}\text{Sr}$ versus N, (b) $^{87}\text{Sr}/^{86}\text{Sr}$ versus [Sr]. An increasing N value representing a greater volume of fluid has reacted with carbonate. The final $^{87}\text{Sr}/^{86}\text{Sr}$ of carbonate is simulated with different initial Sr concentrations of fluid (i.e., $C_{\text{Sr}}^{r0}/C_{\text{Sr}}^{f0} = 3$, 13, 26, and 65). The $(^{87}\text{Sr}/^{86}\text{Sr})^{r0}$ and C_{Sr}^{r0} of the primary carbonates are assigned to be 0.7079 and 1300 ppm, respectively, comparable with those of the least-altered samples from the Monitor Range section. The effective fluid-rock distribution coefficient of Sr (D_{Sr}) and $^{87}\text{Sr}/^{86}\text{Sr}$ of fluid ($(^{87}\text{Sr}/^{86}\text{Sr})^{f0}$) are set to 1 and 0.711[21, 22], respectively.
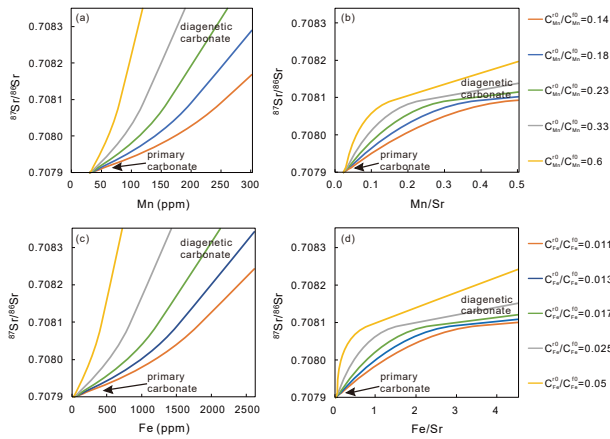
Fig. 5. Modeling results illustrating the evolution of carbonate $^{87}Sr/^{86}Sr$ versus the diagenetic indicators. (a) $^{87}Sr/^{86}Sr$ versus [Mn], (b) $^{87}Sr/^{86}Sr$ versus Mn/Sr, (c) $^{87}Sr/^{86}Sr$ versus [Fe], (d) $^{87}Sr/^{86}Sr$ versus Fe/Sr. $D_{Mn} = 600$, $D_{Fe} = 150$[21, 39]. Other constant parameters are same as in Fig. 4.
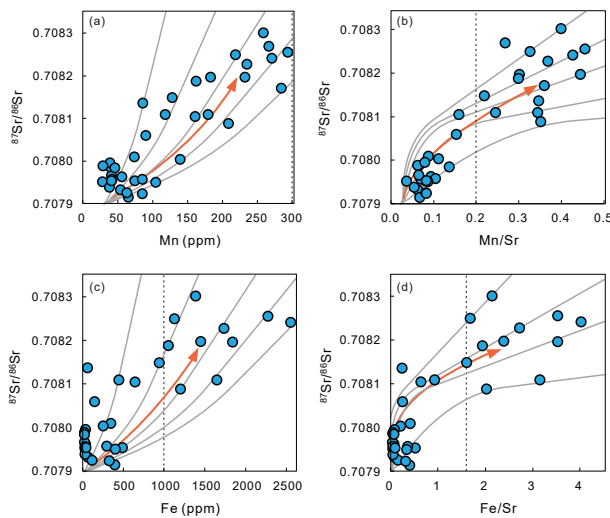

Fig. 6. Crossplots of modeled $^{87}Sr/^{86}Sr$ and geochemical indicators of diagenesis ([Mn], Mn/Sr, [Fe], and Fe/Sr) overlain over data from the Monitor Range section. (a) $^{87}Sr/^{86}Sr$ versus [Mn], (b) $^{87}Sr/^{86}Sr$ versus Mn/Sr, (c) $^{87}Sr/^{86}Sr$ versus [Fe], (d) $^{87}Sr/^{86}Sr$ versus Fe/Sr. The arrows illustrate the evolution direction of $^{87}Sr/^{86}Sr$ with different diagenetic indicators in primary carbonates during diagenesis. The dotted vertical lines denote [Mn] = 300 ppm, Mn/Sr = 0.2, [Fe] = 1000 ppm, and Fe/Sr = 1.6, respectively, representing the threshold of the stricter geochemical criteria for the preservation of Sr isotope systems in carbonates.

and chemical compositions of the coeval seawater, although the samples satisfy the stricter geochemical criteria of preservation of Sr isotope systems (i.e., [Sr] > 300 ppm, [Mn] < 300 ppm, [Fe] < 1000 ppm, Mn/Sr < 0.2, Fe/Sr < 1.6). Second, the comprehensive examination of correlations between $^{87}Sr/^{86}Sr$ and diagenetic indicators ([Mn], [Fe], Mn/Sr, Fe/Sr) and modeling results reveal that the covariations between different elemental proxies provide a geochemical characterization for identifying the effects of diagenesis on carbonate $^{87}Sr/^{86}Sr$ records, highlighting that the combination of geochemical data and numerical modeling has the potential to improve our understanding of the fidelity of carbonate Sr isotope paleoenvironmental proxy.

8　Conclusions

The carbonates from the Late Ordovician Monitor Range section provide important constraints on the importance of diagenetic alteration controlling $^{87}Sr/^{86}Sr$ in bulk carbonate sediments. Analyses of these carbonates, where the $^{87}Sr/^{86}Sr$ of contemporaneous seawater has been well constrained, provide critical insights into our ability to reconstruct the $^{87}Sr/^{86}Sr$ of paleo-seawater from carbonates. The main conclusions of this study are summarized below:

The bulk carbonates from the Monitor Range section record distinctly higher $^{87}Sr/^{86}Sr$ ratios than that of the coeval seawater, suggesting that post-depositional processes have shifted the primary Sr isotopic compositions significantly and cannot be interpreted to represent the long-term variations in seawater $^{87}Sr/^{86}Sr$ values.

The samples exhibit statistically significant positive correlations of $^{87}Sr/^{86}Sr$ with [Mn], [Fe], Mn/Sr, and Fe/Sr, as well as [Mn] with [Fe] and Mn/Sr with Fe/Sr, which is consistent with our modeling results that predict $^{87}Sr/^{86}Sr$ trends to higher values with enrichment of Mn and Fe and depletion of Sr during diagenetic alteration. These observations and modeling results strongly suggest that the radiogenic $^{87}Sr/^{86}Sr$ values of bulk carbonate from the Monitor Range section could be fully attributed to diagenetic resetting.

Our results highlight that although the carbonates meet the stricter geochemical criteria of retention of Sr isotope systems (i.e., [Sr] > 300 ppm, [Mn] < 300 ppm, [Fe] < 1000 ppm, Mn/Sr < 0.2, Fe/Sr < 1.6), their original $^{87}Sr/^{86}Sr$ values may still can be diagenetically altered, urging caution in identifying Sr isotope variations as global until potential diagenetic-related changes can be excluded. We propose that multiple examinations, including correlations between $^{87}Sr/^{86}Sr$ and diagenetic indicators ([Mn], [Fe], Mn/Sr, Fe/Sr) combined with numerical modeling, can be utilized as a useful strategy to demonstrate the preservation of primary seawater $^{87}Sr/^{86}Sr$ values.

Acknowledgements

Conflict of interest

The authors declare that they have no conflict of interest.

Biography

Dongping Hu is currently an Associate Research Fellow at the University of Science and Technology of China (USTC). He received his Ph.D. degree in Geology from USTC in 2017. His research mainly focuses on the reconstruction of paleoenvironmental changes and their potential influences on biological evolution by using multiple stable isotope systematics, such as carbon, sulfur, uranium, and mercury isotopes.

References

[1] Krissansen-Totton J, Buick R, Catling D C. A statistical analysis of the carbon isotope record from the Archean to Phanerozoic and implications for the rise of oxygen. *American Journal of Science,* **2015**, *315* (4): 275–316.

[2] Lu Z L, Lu W Y, Rickaby R E M, et al. Earth history of oxygen and the iprOxy. In: Elements in Geochemical Tracers in Earth System Science. Cambridge, UK: Cambridge University Press, **2020**.

[3] Ling H F, Chen X, Wang D, et al. Cerium anomaly variations in Ediacaran–earliest Cambrian carbonates from the Yangtze Gorges area, South China: Implications for oxygenation of coeval shallow seawater. *Precambrian Research,* **2013**, *225*: 110–127.

[4] Lau K V, Romaniello S J, Zhang F F. The uranium isotope paleoredox proxy. In: Elements in Geochemical Tracers in Earth System Science. Cambridge, UK: Cambridge University Press, **2019**.

[5] Hoffman P F, Kaufman A J, Halverson G P, et al. A Neoproterozoic snowball Earth. *Science,* **1998**, *281* (5381): 1342–1346.

[6] Young S A, Saltzman M R, Foland K A, et al. A major drop in seawater $^{87}Sr/^{86}Sr$ during the Middle Ordovician (Darriwilian): Links to volcanism and climate. *Geology,* **2009**, *37* (10): 951–954.

[7] Capo R C, Depaolo D J. Seawater strontium isotopic variations from 2.5 million years ago to the present. *Science,* **1990**, *249* (4964): 51–55.

[8] Sedlacek A R C, Saltzman M R, Thomas A, et al. $^{87}Sr/^{86}Sr$ stratigraphy from the Early Triassic of Zal, Iran: Linking temperature to weathering rates and the tempo of ecosystem recovery. *Geology,* **2014**, *42* (9): 779–782.

[9] Blum J D, Erel Y. A silicate weathering mechanism linking increases in marine $^{87}Sr/^{86}Sr$ with global glaciation. *Nature,* **1995**, *373* (6513): 415–418.

[10] Halverson G P, Dudás F Ö, Maloof A C, et al. Evolution of the $^{87}Sr/^{86}Sr$ composition of Neoproterozoic seawater. *Palaeogeography, Palaeoclimatology, Palaeoecology,* **2007**, *256* (3–4): 103–129.

[11] Swanson-Hysell N L, Macdonald F A. Tropical weathering of the Taconic orogeny as a driver for Ordovician cooling. *Geology,* **2017**, *45* (8): 719–722.

[12] Prokoph A, Shields G A, Veizer J. Compilation and time-series analysis of a marine carbonate $\delta^{18}O$, $\delta^{13}C$, $^{87}Sr/^{86}Sr$ and $\delta^{34}S$ database through Earth history. *Earth-Science Reviews,* **2008**, *87* (3 –4): 113–133.

[13] Paytan A, Griffith E M, Eisenhauer A, et al. A 35-million-year record of seawater stable Sr isotopes reveals a fluctuating global carbon cycle. *Science,* **2021**, *371* (6536): 1346–1350.

[14] Wang W Q, Katchinoff J A R, Garbelli C, et al. Revisiting the Permian seawater $^{87}Sr/^{86}Sr$ record: New perspectives from brachiopod proxy data and stochastic oceanic box models. *Earth-Science Reviews,* **2021**, *218*: 103679.

[15] Edwards C T, Saltzman M R, Leslie S A, et al. Strontium isotope ($^{87}Sr/^{86}Sr$) stratigraphy of Ordovician bulk carbonate: Implications for preservation of primary seawater values. *Geological Society of America Bulletin,* **2015**, *127* (9-10): 1275–1289.

[16] Saltzman M R, Edwards C T, Leslie S A, et al. Calibration of a conodont apatite-based Ordovician $^{87}Sr/^{86}Sr$ curve to biostratigraphy and geochronology: Implications for stratigraphic resolution. *Geological Society of America Bulletin,* **2014**, *126* (11 –12): 1551–1568.

[17] Veizer J, Buhl D, Diener A, et al. Strontium isotope stratigraphy: potential resolution and event correlation. *Palaeogeography, Palaeoclimatology, Palaeoecology,* **1997**, *132* (1-4): 65–77.

[18] Burke W H, Denison R E, Hetherington E A, et al. Variation of seawater $^{87}Sr/^{86}Sr$ throughout Phanerozoic time. *Geology,* **1982**, *10* (10): 516–519.

[19] McArthur J M, Howarth R J, Shields G A, et al. Strontium isotope stratigraphy. In: Geologic Time Scale 2020. Amsterdam: Elsevier, **2020**: 211–238.

[20] Banner J L, Hanson G N. Calculation of simultaneous isotopic and trace element variations during water-rock interaction with applications to carbonate diagenesis. *Geochimica et Cosmochimica Acta,* **1990**, *54* (11): 3123–3137.

[21] Jacobsen S B, Kaufman A J. The Sr, C and O isotopic evolution of Neoproterozoic seawater. *Chemical Geology,* **1999**, *161*: 37–57.

[22] Banner J L. Application of the trace-element and isotope geochemistry of strontium to studies of carbonate diagenesis. *Sedimentology,* **1995**, *42* (5): 805–824.

[23] Finnegan S, Bergmann K, Eiler J M, et al. The magnitude and duration of Late Ordovician–Early Silurian glaciation. *Science,* **2011**, *331* (6019): 903–906.

[24] Trotter J A, Williams I S, Barnes C R, et al. Did cooling oceans trigger Ordovician biodiversification? Evidence from conodont thermometry. *Science,* **2008**, *321* (5888): 550–554.

[25] Finney S C, Berry W B N, Cooper J D, et al. Late Ordovician mass extinction: A new perspective from stratigraphic sections in central Nevada. *Geology,* **1999**, *27* (3): 215–218.

[26] Finney S C, Cooper J D, Berry W B N. Late Ordovician mass extinction: Sedimentologic, cyclostratigraphic, and biostratigraphic records from platform and basin successions, central Nevada. In: Proterozoic to Recent Stratigraphy, Tectonics, and Volcanology, Utah, Nevada, Southern Idaho, and Central Mexico. Provo, UT: Brigham Young University, **1997**: 79–104.

[27] Saltzman M R, Young S A. Long-lived glaciation in the Late Ordovician? Isotopic and sequence-stratigraphic evidence from western Laurentia. *Geology,* **2005**, *33* (2): 109–112.

[28] LaPorte D F, Holmden C, Patterson W P, et al. Local and global perspectives on carbon and nitrogen cycling during the Hirnantian glaciation. *Palaeogeography, Palaeoclimatology, Palaeoecology,* **2009**, *276* (1–4): 182–195.

[29] Jones D S, Martini A M, Fike D A, et al. A volcanic trigger for the Late Ordovician mass extinction? Mercury data from south China and Laurentia. *Geology,* **2017**, *45* (7): 631–634.

[30] Jones D S, Creel R C, Rios B A. Carbon isotope stratigraphy and correlation of depositional sequences in the Upper Ordovician Ely Springs Dolostone, eastern Great Basin, USA. *Palaeogeography, Palaeoclimatology, Palaeoecology,* **2016**, *458*: 85–101.

[31] Kozik N P, Gill B C, Owens J D, et al. Geochemical records reveal protracted and differential marine redox change associated with Late Ordovician climate and mass extinctions. *AGU Advances,* **2022**, *3* (1): e2021AV000563.

[32] Finney S C, Berry W B N, Cooper J D. The influence of denitrifying seawater on graptolite extinction and diversification during the Hirnantian (latest Ordovician) mass extinction event. *Lethaia,* **2007**, *40* (3): 281–291.

[33] Lin J, Liu Y S, Chen H H, et al. Review of high-precision Sr isotope analyses of low-Sr geological samples. *Journal of Earth Science,* **2015**, *26* (5): 763–774.

[34] Goldman D, Sadler P M, Leslie S A. The Ordovician period. In: Geologic Time Scale 2020. Amsterdam: Elsevier, **2020**: 631–694.

[35] Denison R E, Koepnick R B, Fletcher A, et al. Criteria for the retention of original seawater $^{87}Sr/^{86}Sr$ in ancient shelf limestones. *Chemical Geology,* **1994**, *112* (1-2): 131–143.

[36] Tucker M E, Wright V P. Carbonate Sedimentology. Oxford: Blackwell Scientific, **1990**.

[37] Brand U, Veizer J. Chemical diagenesis of a multicomponent carbonate system – 2: Stable isotopes. *Journal of Sedimentary Research,* **1981**, *51* (3): 987–997.

[38] Kaurova O K, Ovchinnikova G V, Gorokhov I M. U-Th-Pb systematics of precambrian carbonate rocks: Dating of the formation and transformation of carbonate sediments. *Stratigraphy and Geological Correlation,* **2010**, *18* (3): 252–268.

[39] Brand U, Veizer J. Chemical diagenesis of a multicomponent carbonate system – 1: Trace elements. *Journal of Sedimentary Research,* **1980**, *50* (4): 1219–1236.

[40] Wang W Q, Garbelli C, Zheng Q F, et al. Permian $^{87}Sr/^{86}Sr$ chemostratigraphy from carbonate sequences in South China. *Palaeogeography, Palaeoclimatology, Palaeoecology,* **2018**, *500*: 84–94.

[41] Kuznetsov A B, Semikhatov M A, Gorokhov I M, et al. Sr isotopic composition in carbonates of the Karatau Group, southern Urals, and standard curve of $^{87}Sr/^{86}Sr$ variations in the Late Riphean ocean.

Stratigraphy and Geological Correlation, **2003**, *11* (5): 415–449.

[42] Rud' ko S V, Kuznetsov A B, Piskunov V K. Sr isotope chemostratigraphy of Upper Jurassic carbonate rocks in the Demerdzhi Plateau (Crimean Mountains). *Stratigraphy and Geological Correlation,* **2014**, *22* (5): 494–506.

[43] Qing H R, Barnes C R, Buhl D, et al. The strontium isotopic composition of Ordovician and Silurian brachiopods and conodonts: Relationships to geological events and implications for coeval seawater. *Geochimica et Cosmochimica Acta,* **1998**, *62* (10):

1721–1733.

[44] Shields G A, Carden G A F, Veizer J, et al. Sr, C, and O isotope geochemistry of Ordovician brachiopods: a major isotopic event around the Middle-Late Ordovician transition. *Geochimica et Cosmochimica Acta,* **2003**, *67* (11): 2005–2025.

[45] Bergström S M, Chen X, GutiÉrrez-Marco J C, et al. The new chronostratigraphic classification of the Ordovician System and its relations to major regional series and stages and to δ^{13}C chemostratigraphy. *Lethaia,* **2009**, *42* (1): 97–107.